THE JOURNAL OF BIOLOGICAL CHEMISTRY VOL. 285, NO. 48, pp. 37927–37938, November 26, 2010

$InsP_3R$-associated cGMP Kinase Substrate Determines Inositol 1,4,5-Trisphosphate Receptor Susceptibility to Phosphoregulation by Cyclic Nucleotide-dependent Kinases*[S]

Received for publication, July 27, 2010, and in revised form, September 1, 2010 Published, JBC Papers in Press, September 27, 2010, DOI 10.1074/jbc.M110.168989

Wataru Masuda[‡], Matthew J. Betzenhauser[§], and David I. Yule[¶1]

From the [¶]Department of Pharmacology and Physiology, University of Rochester Medical School, Rochester, New York 14642, the [§]Department of Physiology and Cellular Biophysics, Columbia University Medical School, New York, New York 10032, and the [‡]Department of Biosciences, Kyushu Dental College, 2-6-1 Manazuru, Kokurakita-ku, Kitakyushu-shi, Fukuoka 803-8580, Japan

Ca^{2+} release through inositol 1,4,5-trisphosphate receptors ($InsP_3R$) can be modulated by numerous factors, including input from other signal transduction cascades. These events shape the spatio-temporal characteristics of the Ca^{2+} signal and provide fidelity essential for the appropriate activation of effectors. In this study, we investigate the regulation of Ca^{2+} release via $InsP_3R$ following activation of cyclic nucleotide-dependent kinases in the presence and absence of expression of a binding partner $InsP_3R$-associated cGMP kinase substrate (IRAG). cGMP-dependent kinase (PKG) phosphorylation of only the S2+ $InsP_3R$-1 subtype resulted in enhanced Ca^{2+} release in the absence of IRAG expression. In contrast, IRAG bound to each $InsP_3R$ subtype, and phosphorylation of IRAG by PKG attenuated Ca^{2+} release through all $InsP_3R$ subtypes. Surprisingly, simply the expression of IRAG attenuated phosphorylation and inhibited the enhanced Ca^{2+} release through $InsP_3R$-1 following cAMP-dependent protein kinase (PKA) activation. In contrast, IRAG expression did not influence the PKA-enhanced activity of the $InsP_3R$-2. Phosphorylation of IRAG resulted in reduced Ca^{2+} release through all $InsP_3R$ subtypes during concurrent activation of PKA and PKG, indicating that IRAG modulation is dominant under these conditions. These studies yield mechanistic insight into how cells with various complements of proteins integrate and prioritize signals from ubiquitous signaling pathways.

Cells express an array of cell surface receptors that couple neurotransmitters, hormones, and growth factors to cellular responses. *In vivo*, cells are seldom exposed to single modulating agents, and thus initiation of multiple signal transduction pathways concurrently is the norm. As a result of interaction between individual signal transduction cascades, one pathway can markedly influence the activity of another; the overall cellular response will therefore be determined by the integration and prioritization of these multiple inputs. Cell surface receptors coupled to a release of intracellular Ca^{2+} are expressed in all mammalian cells, and this pathway is a particularly rich source of potential interaction between distinct signal transduction systems (1, 2). The Ca^{2+} rise can initiate further signaling cascades, for instance by influencing the generation and metabolism of other second messengers, including cAMP and cGMP (3, 4). Importantly, the precise kinetic and spatial properties of the Ca^{2+} signal are pivotal to the appropriate stimulation of effectors, and thus regulatory input modulating the activity of the Ca^{2+} handling machinery itself is central to the spatio-temporal "shaping" of the Ca^{2+} signal (5).

A primary locus for modifying the characteristics of the intracellular Ca^{2+} signal is through regulating the activity of the $InsP_3R$[2] family of Ca^{2+} release channels. $InsP_3R$ are encoded by three genes, leading to the expression of three distinct proteins ($InsP_3R$-1, $InsP_3R$-2, and $InsP_3R$-3) (6–8). Additional diversity at the protein level is generated from numerous splice variants of the $InsP_3R$-1 and $InsP_3R$-2 and the formation of heterotetrameric channel proteins (9). Ca^{2+} release is allosterically regulated by a diverse array of modulatory events allowing input from other intracellular factors or events. These include the levels of intracellular Ca^{2+}, ATP levels, phosphorylation events, and binding of protein partners (2, 9–11). Outside of the conserved NH_2-terminal $InsP_3$ binding pocket and the COOH-terminal channel domain, the primary sequence of the individual proteins is quite divergent, allowing for potential $InsP_3R$ subtype-specific regulation of Ca^{2+} release. This regulation, along with the particular complement of $InsP_3R$ expressed, is thought to make a significant contribution to defining the particular Ca^{2+} signals observed in individual cell types.

A relatively well studied mode of regulation of $InsP_3R$ activity occurs following the phosphorylation of the receptor by

* This work was supported, in whole or in part, by National Institutes of Health Grants RO1-DK05458 and RO1-DE14756.

[S] The on-line version of this article (available at http://www.jbc.org) contains supplemental Figs. 1–3.

[1] To whom correspondence should be addressed: Dept. of Pharmacology and Physiology, University of Rochester Medical School, 601 Elmwood Ave., Rochester, NY 14642. Tel.: 585-273-2154; Fax: 585-273-2154; E-mail: David_Yule@urmc.rochester.edu.

[2] The abbreviations used are: $InsP_3R$, inositol 1,4,5-trisphosphate receptor(s); $InsP_3$, inositol 1,4,5-trisphosphate; IRAG, $InsP_3R$-associated cGMP kinase substrate; CCh, carbachol; M3R, human muscarinic M3R; PKA, protein kinase A; PKG, cGMP-dependent kinase(s); cBIMPS, 5,6-dichloro-1-β-D- ribofuranosylbenzylimadazole-3′,5′-cyclic monophosphorothioate; PET-cGMP, 8-bromo-β-phenyl-1,N^2-ethenoguanosine-3′,5′-cyclic monophosphorothioate; Rp-8-Br-PET-cGMP, 8-bromo-β-phenyl-1,N^2-ethenoguanosine- 3′,5′-cyclic monophosphorothioate, Rp-isomer.

cAMP-dependent protein kinase (PKA) (11), a primary interaction or point of "cross-talk" between cascades that increase Ca^{2+} or cAMP. PKA has been shown to phosphorylate defined serine residues on each isoform of $InsP_3R$ (12–14) and clearly enhances the single channel activity of at least the $InsP_3R$-2 (12) and $InsP_3R$-1 (15, 16). In contrast, the Ca^{2+} release activity of $InsP_3R$-3 is apparently unaffected by PKA phosphorylation (17). The increased $InsP_3R$ activity has been proposed to be physiologically important for processes as diverse as neuronal plasticity and fluid secretion from salivary epithelia (15, 18).

cGMP-dependent kinases (PKG) phosphorylate similar consensus sequences on substrates as PKA (RR*X*(S/T) or R*XX*(S/T), where R is basic) and thus would be expected to have functional effects similar to those of PKA. PKG can be activated following ligand binding of receptors with intrinsic guanylate cyclase activity or as a consequence of the action of nitric oxide on soluble guanylate cyclases (19). An elevation in cAMP can also lead to PKG activation either directly or indirectly by increasing cGMP levels through substrate competition at the level of shared phosphodiesterases. When the functional effects on $InsP_3R$-1 were studied directly, PKG phosphorylation of identical sites regulated by PKA resulted, as expected, in a marked enhancement of the neuronal S2+ $InsP_3R$-1 activity (20). The alternatively spliced S2− $InsP_3R$-1 variant, the major $InsP_3R$-1 splice variant expressed outside the neural system, resulting in 40 amino acids excised between phosphorylation sites, was not subject to regulation by PKG (20). These data indicate that all PKA consensus sequences are not necessarily PKG substrates. No data are available regarding direct effects of PKG on $InsP_3R$-2 and $InsP_3R$-3.

Elevations in cGMP have, however, been predominantly linked to an attenuation of Ca^{2+} signaling (21–24); this may reflect either PKG phosphorylation of $InsP_3R$-2/-3 or PKG-dependent phosphorylation of other substrates. For example, PKG can also influence the activity of $InsP_3R$ by phosphorylation of a binding partner termed $InsP_3R$-associated PKG substrate (IRAG) (25, 26). This protein constitutively binds to both $InsP_3R$-1 and PKG1β, and the tight association between proteins allows for efficient targeted phosphoregulation. In smooth muscle and platelets, IRAG is phosphorylated on serine 696 and leads to decreased $InsP_3$-induced Ca^{2+} release (27). Although it is not known if IRAG interacts with all subtypes of $InsP_3R$ or if its expression is ubiquitous, this mechanism may reconcile earlier observations of decreased Ca^{2+} release following PKG and PKA activation in various tissues (22, 24, 28).

The goal of the present study was to further investigate the regulation of Ca^{2+} release by PKA and PKG. By using an expression system that is functionally null for both $InsP_3R$ and IRAG, we define the particular $InsP_3R$ that are subject to direct regulation by PKG and indirect regulation by interaction through IRAG. Furthermore, because PKG and PKA are commonly activated concurrently, we define the conditions and the molecular mechanism by which a particular mode of regulation is specified and is dominant at the cellular level.

EXPERIMENTAL PROCEDURES

Materials—PET-cGMP, 8-bromo-cyclic GMP, Rp-8-Br-PET-cGMP, and cBIMPS were purchased from BIOLOG (Bremen, Germany). All other chemicals were purchased from Sigma. A rabbit polyclonal antibody designed against a specific sequence in the rat $InsP_3R$-2 extreme COOH terminus (α-$InsP_3R$-2-CT; ^{2686}GFLGSNTPHENHHMPPH^{2702}) was generated by Pocono Rabbit Farms and Laboratories (Canadensis, PA) (29). A rabbit polyclonal antibody against the region surrounding phosphorylated Ser^{937} of mouse $InsP_3R$-2(Ser^{937}) (^{934}SRGpSIFPVSVPDAC^{946}, where pS represents phosphoserine) was generated by Quality Controlled Biochemicals (Hopkinton, MA) (12). The remaining antibodies were commercially available as follows: α-$InsP_3R$-1 rabbit polyclonal antibody (Calbiochem); α-phospho-$InsP_3R$-1(Ser^{1756}) rabbit polyclonal antibody (30, 31) (Cell Signaling, Danvers, MA); α-$InsP_3R$-3 mouse monoclonal antibody (BD Transduction Laboratories); α-PKG1α/β rabbit polyclonal antibody (Santa Cruz Biotechnology, Inc., Santa Cruz, CA); α-FLAG mouse monoclonal antibody (Sigma), α-GFP mouse (monoclonal antibody) (Roche Applied Science).

Generation and Transfection of Expression Constructs—A vector containing the full-length cDNA for IRAG was obtained from the RIKEN cDNA collection. The open reading frame was cloned by PCR into pCI-Neo-EGFP. To create the deletion mutant (Δ residues 460–506) of IRAG (IRAGΔE12), we used the QuikChange Lightning kit (Stratagene). Correct incorporation of mutations was confirmed by DNA sequencing. COS-7 cells were cultured in Dulbecco's modified Eagle's medium with 10% fetal bovine serum, penicillin, and streptomycin at 37 °C. Transient transfections were performed using Lipofectamine 2000 (Invitrogen) according to the manufacturer's directions. Cells were harvested 1 day after transfection. cDNA was transfected into DT40 cells stably expressing rat $InsP_3R$-1, mouse $InsP_3R$-2, and rat $InsP_3R$-3 cells (for details of generation of stable cell lines, see Ref. 29) by an electroporation-based protocol using an Amaxa Nucleofector® system using 5 μg of each cDNA (Amaxa, Cologne, Germany) following the manufacturer's instructions (kit T, program B23).

Immunoprecipitation and Immunoblotting—Transfected COS-7 cells were incubated in lysis buffer (50 mM Tris, 150 mM NaCl, 10 mM EDTA, 1% Triton X-100, pH 7.4, adjusted with NaOH), and the preparation was centrifuged at 10,000 × *g* for 5 min at 4 °C. The resulting supernatant was incubated with 30 μl of protein G-agarose (Santa Cruz Biotechnology, Inc.) for 1 h, at 4 °C, to control nonspecific binding to the protein G-agarose. The clarified supernatant was incubated with 2 μg of α-GFP monoclonal antibody (Roche Applied Science) or 2.5 μg of α-FLAG monoclonal antibody (Sigma) for 1 h. The mixture was supplemented with 50 μl of protein G-agarose and incubated for another 1 h at 4 °C. The agarose was washed three times with the lysis buffer, and then immune complex-associated proteins were resolved by 5% SDS-PAGE and electrophoretically transferred to nitrocellulose membranes. The membranes were incubated with primary antibody and then with secondary antibody. The bands were visu-

alized by enhanced chemiluminescence (PerkinElmer Life Sciences).

Analysis of $InsP_3R$ Phosphorylation—COS-7 cells transfected with cDNA encoding $InsP_3R$, IRAG(GFP) or IRAGΔE12(GFP), and PKG1β were treated with 1 μM forskolin and 200 μM isobutylmethylxanthine for 10 min at room temperature. Cell lysates were harvested by the addition of ice-cold 2× SDS-PAGE sample loading buffer. Proteins were then separated by SDS-PAGE. Phosphorylated Ser^{1755} in $InsP_3R$-1 and Ser^{937} in $InsP_3R$-2 were detected with α-phospho-$InsP_3R$-1(Ser^{1756}) (30, 31) rabbit polyclonal antibody or α-$InsP_3R$-2(Ser^{937}) (12), respectively, by Western blotting. Blots were stripped and reprobed with α-$InsP_3R$-1 or α-$InsP_3R$-2-CT, α-PKG1α/b polyclonal antibody, and α-GFP monoclonal antibody. The blots were analyzed by densitometry using ImageJ software.

Digital Imaging of $[Ca^{2+}]_i$ in DT40 Cells—Imaging was performed as described previously (32). Briefly, DT40 cells were loaded with 2 μM fura-2/AM at room temperature for 10 min. Fura-2-loaded cells were allowed to adhere to a glass coverslip forming the bottom of a perfusion chamber. Cells were perfused in HEPES-buffered physiological saline containing 137 mM NaCl, 0.56 mM $MgCl_2$, 4.7 mM KCl, 1 mM Na_2HPO_4, 10 mM HEPES, 5.5 mM glucose, and 1.26 mM $CaCl_2$ at pH 7.4. Imaging was performed using an inverted Olympus IX71 microscope using a ×40 oil immersion objective lens (UApo/340; numerical aperture 1.35). Fura-2-loaded cells were excited alternately with light at 340 and 380 nm by using a monochrometer-based illumination system (TILL Photonics), and the emission at 510 nm was captured by a digital frame transfer CCD camera controlled by the Vision suite of software. In experiments where GFP-tagged IRAG (IRAG(GFP)) or IRAGΔE12 (IRAGΔE12(GFP)) was transiently expressed, GFP fluorescence was detected by excitation at 488 nm and monitoring the emission at >500 nm and was used to select transfected cells. In other experiments, cDNA encoding HcRed was included to select transfected cells. HcRed fluorescence was detected by excitation at 560 nm and observing the emission at >600 nm.

Statistical Analysis—Data are presented as mean ± S.E. Data were subjected to one-way analysis of variance. Statistical significance is indicated where $p < 0.05$.

RESULTS

IRAG Physically Interacts with All $InsP_3R$ Subtypes—Schlossman and colleagues (26, 27, 33) have reported that IRAG physically interacts with and regulates the activity of $InsP_3R$-1 both *in vivo* and *in vitro*. Because the binding determinants of IRAG in $InsP_3R$-1 are not known, the likelihood of an interaction with other $InsP_3R$ subtypes is difficult to predict. In order to establish if IRAG can potentially modulate other $InsP_3R$ family members and splice variants, experiments were first performed to ascertain whether IRAG physically interacts with all subtypes of $InsP_3R$ and is capable of forming a tertiary complex with PKG1β. COS-7 cells were chosen for these experiments because of the ability to achieve high levels of heterologous protein expression together with low endogenous $InsP_3R$ expression (12, 31, 34). Following transfection

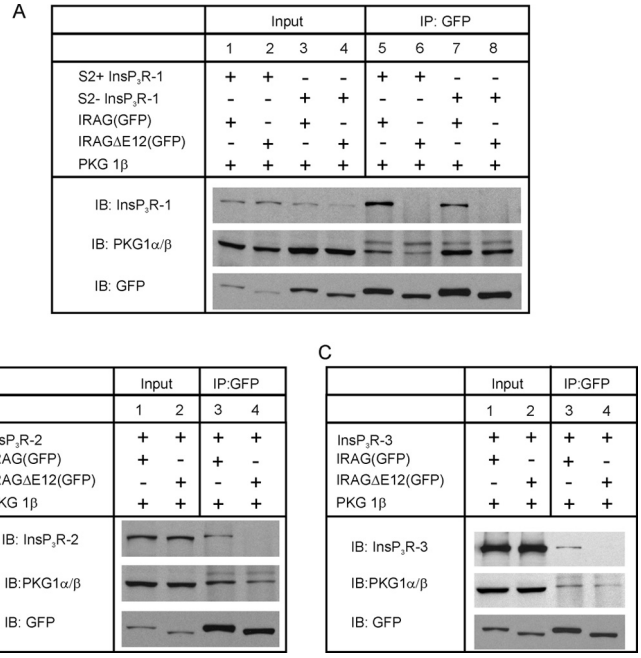

FIGURE 1. **Interaction of $InsP_3R$ with IRAG and PKG1β in COS-7 cells.** The proteins indicated in the figure were transiently expressed in COS-7 cells. Immune complexes were captured by immunoprecipitation (*IP*) from cell lysates with α-GFP monoclonal antibody. In *A*, *lanes 1–4* show the input, representing 5% of the lysate prior to immunoprecipitation. Immunoprecipitated samples were subjected to Western blot analysis (*IB*) for detection of S2+/S2− $InsP_3R$-1, PKG1β, and IRAG(GFP) or IRAGΔE12(GFP) (*lanes 5–8*). Both splice variants of $InsP_3R1$ were co-immunoprecipitated only in the presence of full-length IRAG (*lanes 5* and *7*). In contrast, PKG1β was co-immunoprecipitated with antibody independent of IRAG type. In *B*, immunoprecipitated samples were subjected to Western blot analysis for detection of $InsP_3R$-2, PKG1β, and IRAG(GFP) or IRAGΔE12(GFP). *Lanes 1* and *2* show input representing 5% of the sample. $InsP_3R$-2 was co-immunoprecipitated with antibody only in the presence of full-length IRAG (*lane 3*). In contrast, PKG1β was co-immunoprecipitated with antibody independent of IRAG type. In *C*, immunoprecipitated samples were subjected to Western blot analysis for detection of $InsP_3R$-3, PKG1β, and IRAG(GFP) or IRAGΔE12(GFP). *Lanes 1* and *2* show input representing 5% of the sample. $InsP_3R$-3 was co-immunoprecipitated with antibody only in the presence of wild type IRAG (*lane 3*). In contrast, PKG1β was co-immunoprecipitated with antibody independent of IRAG type. Results presented are representative of at least three independent similar experiments.

with $InsP_3R$ subtypes, GFP-tagged IRAG and PKG1β immune complexes were isolated from cell lysates by incubation with α-GFP antisera as detailed under "Experimental Procedures." Similar experiments were performed in cells transfected with a GFP-IRAG construct (IRAGΔE12(GFP)), which lacks the coiled-coil domain of IRAG necessary for interaction with $InsP_3R$-1 (27, 33). In Fig. 1*A*, a representative blot is presented, which shows that immunoprecipitation with α-GFP antibody captures both S2+ and S2− $InsP_3R$-1 and PKG1β when full-length IRAG(GFP) is co-expressed (*lanes 5* and *7*, respectively). In contrast, in cells expressing IRAGΔE12(GFP), PKG1β but not $InsP_3R$-1 was recovered from the lysates following IP (*lanes 6* and *8*). Similar experiments were performed to determine if $InsP_3R$-2 and $InsP_3R$-3 interact in an analogous fashion with IRAG and PKG1β. The *lower panels* of Fig. 1 demonstrate that immunoprecipitation of full-length IRAG(GFP) robustly captures $InsP_3R$-2 (Fig. 1*B*) or $InsP_3R$-3 (Fig. 1*C*) and PKG1β, whereas immunoprecipitation of IRAGΔE12(GFP) does not.

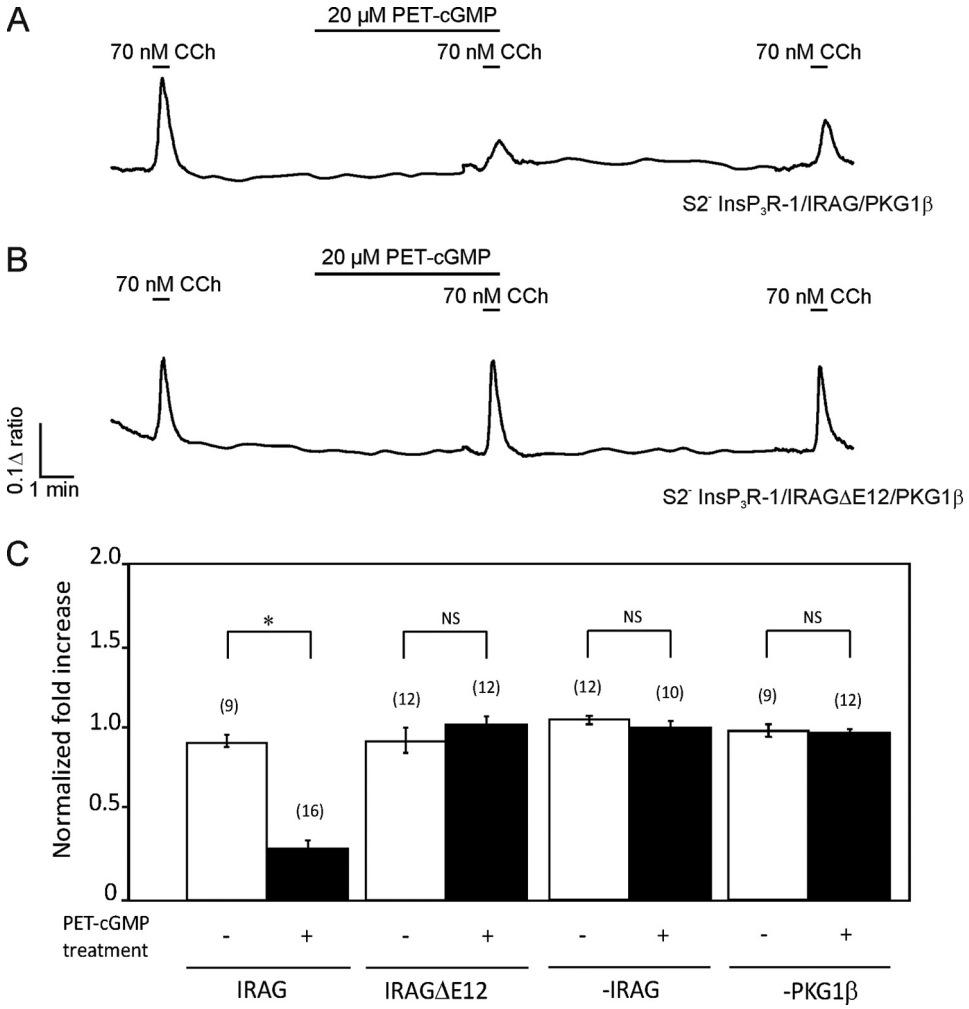

FIGURE 2. **Ca^{2+} release through S2− $InsP_3R$-1 is attenuated by PKG activation in cells expressing IRAG/PKG1β.** DT40-3KO cells stably expressing S2− $InsP_3R$-1 were transfected with cDNA encoding M3R, IRAG(GFP) in *A* or IRAGΔE12(GFP) in *B*, and PKG1β. Transient Ca^{2+} release was induced by 30-s exposure to 70 nM CCh. In *A*, treatment with 20 μM PET-cGMP resulted in a markedly attenuated CCh-induced Ca^{2+} release in the presence of wild type IRAG. In *B*, no effect of incubation with PET-cGMP was observed in the presence of IRAGΔE12. *C*, pooled data. In each set of experiments, experimental runs were performed without PKA/PKG activators/inhibitors to gauge the reproducibility of the agonist responses. Data in the *open bars* represent the -fold change of the second response compared with the first response in the absence of treatment. The *filled bars* show the normalized -fold increase of the second peak over the first peak for the indicated experimental condition. *Columns* represent mean ± S.E. (*error bars*). **, $p < 0.0001$; *NS*, not statistically significant. The number of cells in each condition is indicated in *parentheses*.

PKG1β Phosphorylation of IRAG Modulates $InsP_3$-induced Ca^{2+} Release via $InsP_3R$-1—Next, experiments were performed to determine if the interaction of IRAG/PKG1β with individual $InsP_3R$ subtypes modulates Ca^{2+} release. By virtue of targeted deletion of both copies of the three chicken $InsP_3R$ genes, the DT40-3KO pre-B lymphocyte cell line is a unique experimental platform to monitor the function of defined populations of mammalian $InsP_3R$ in an unambiguously null background (35). Our previous studies have generated stable cell lines expressing individual mammalian $InsP_3R$ splice variants and subtypes (29, 32, 36). To monitor the effects of PKG activation on Ca^{2+} release, these lines were transfected with muscarinic M3 receptor (M3R), together with IRAG constructs and PKG1β. Ca^{2+} release was monitored in fura-2-loaded cells following stimulation of M3R with low concentrations of CCh. This paradigm has been shown to be a convenient and relatively faithful reflection of Ca^{2+} release, given that little desensitization of the response is observed over multiple exposures to agonist, and the initial peak height is largely independent of Ca^{2+} influx (16, 31). Initially, experiments were performed with DT40-3KO cells stably expressing the S2− peripheral splice variant of $InsP_3R$-1 and transiently expressing M3R, IRAG(GFP), and PKG1β. Ca^{2+} release was initiated by brief exposure to a low concentration of CCh, and following agonist washout, the cells were incubated for 5 min with the cell-permeable and phosphodiesterase-resistant cGMP analog PET-cGMP and subsequently re-stimulated with CCh. As shown in Fig. 2*A* (pooled data in Fig. 2*C*), activation of PKG resulted in a marked inhibition of the CCh-induced Ca^{2+} signal, which was partially reversible upon removal of the cGMP analog. The inhibition of Ca^{2+} release was dependent on both the expression of PKG1β and IRAG because failing to express either protein abrogated the response (Fig. 2*C*). The current experiments are consistent with our earlier data, which suggested that S2− $InsP_3R$-1 are not a direct substrate for PKG (20, 31). Furthermore, the inhibition was dependent on the interaction between IRAG and S2-$InsP_3R$-1 because no attenuation of the CCh-induced Ca^{2+}

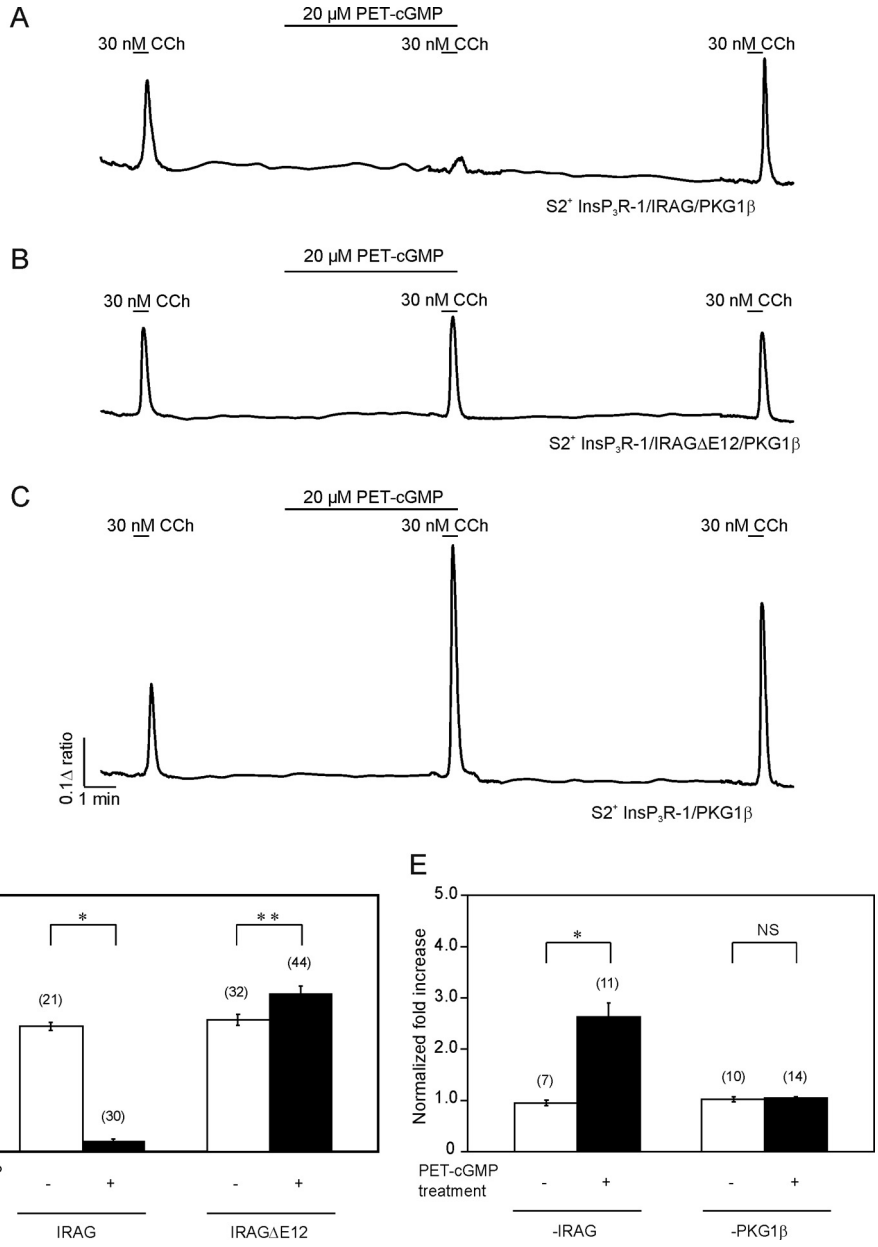

FIGURE 3. **Ca^{2+} release through S2+ InsP$_3$R-1 is attenuated by PKG activation in cells expressing IRAG/PKG1β.** DT40-3KO cells stably expressing S2+ InsP$_3$R-1 were transfected with cDNA encoding M3R, IRAG(GFP) in *A* or IRAGΔE12(GFP) in *B*, and PKG1β. In *A*, treatment with 20 μM PET-cGMP resulted in a markedly attenuated CCh-induced Ca^{2+} release in the presence of full-length IRAG. In contrast, in *B*, in cells expressing IRAGΔ12(GFP), a small but statistically significant increase in CCh-induced Ca^{2+} release was observed. In *C*, in the absence of IRAG expression, PET-cGMP resulted in a marked potentiation of the CCh-induced Ca^{2+} release. *D* and *E* show the pooled data in the presence and absence of full-length IRAG expression, respectively. Data in the *open bars* represent the -fold change of the second response compared with the first response in the absence of treatment. The *filled bars* show the normalized -fold increase of the second peak over the first peak for the indicated experimental condition. *Columns* represent mean ± S.E. (*error bars*). **, $p < 0.0001$; ***, $p < 0.05$; *NS*, not statistically significant. The number of cells in each condition is indicated in *parentheses*.

signal following PET-cGMP exposure was observed in cells expressing IRAGΔE12(GFP) (Fig. 2*B*). These data indicate the importance of the InsP$_3$R-1·IRAG·PKG1β complex and that DT40-3KO cells are functionally null for IRAG and PKG1β in the absence of ectopic expression.

Similar experiments were performed in cells stably expressing the S2+ neuronal InsP$_3$R-1 splice variant. PET-cGMP treatment of cells transiently expressing M3R, IRAG(GFP), and PKG1β resulted in a marked inhibition of the CCh-induced Ca^{2+} rise (Fig. 3, *A* and pooled data in *D*). Again, the attenuation of Ca^{2+} release was dependent on the expression of PKG1β and binding of IRAG to the InsP$_3$R-1 (Fig. 3, *B* and *D*). In contrast, in the absence of IRAG, PET-cGMP incubation led to a striking enhancement of the CCh-induced Ca^{2+} signal (Fig. 3, *C* and pooled data in *E*), presumably as a result of the fact that S2+ InsP$_3$R-1 is a direct substrate for PKG and phosphorylation of Ser^{1755} of S2+ InsP$_3$R results in a marked increase in the open probability of the receptor (16). A small but statistically significant increase in Ca^{2+} release was also observed in cells expressing IRAGΔE12(GFP) and PKG1β (Fig. 3, *B* and *D*). This observation is also consistent with direct phosphorylation of S2+ InsP$_3$R-1; however, the finding

that this effect is smaller than observed in the absence of IRAG may reflect the fact that IRAGΔE12(GFP) retains PKG1β binding (27) and thus may sequester a fraction of the kinase from other substrates. The data in Fig. 3*A* also suggest that the inhibitory effect of phosphorylation of IRAG is dominant over any positive effect of direct phosphorylation of S2+ InsP$_3$R-1.

PKG1β Phosphorylation of IRAG Modulates InsP$_3$-induced Ca^{2+} Release via InsP$_3$R-2 and -3—Next, experiments addressed whether binding of IRAG to InsP$_3$R-2 and InsP$_3$R-3 is translated into modulation of Ca^{2+} release through these particular receptors. Cells stably expressing mouse InsP$_3$R-2 were transfected with M3R, PKG1β, and IRAG(GFP). Exposure of these cells to PET-cGMP resulted in a considerable attenuation of the CCh-induced Ca^{2+} signal, which again was fully reversible upon removal of the cGMP analog (Fig. 4, *A* and pooled data in *D*). This effect was dependent on PKG activity because the extent of inhibition was significantly reduced by concurrent exposure to the PKG inhibitor Rp-8-Br-PET-cGMP (Fig. 4, *B* and *D*). In a similar fashion to InsP$_3$R-1, the reduction of the Ca^{2+} signal was dependent on the expression and binding of IRAG (Fig. 4, *C* and *D*). Further, in cells expressing PKG1β in the absence of IRAG, no effect of PKG activation was observed. These data indicate that, despite InsP$_3$R-2 being a substrate for PKA, InsP$_3$R-2 is unlikely to be a direct substrate for PKG. Experiments were also performed to gauge the impact of IRAG modulation of Ca^{2+} signaling during Ca^{2+} oscillations, considered a more physiological mode of signaling. Ca^{2+} oscillations initiated by continued exposure to low [CCh] in cells expressing M3R, IRAG(GFP), and PKG1β were rapidly inhibited by activation of PKG (supplemental Fig. 1*A*). This inhibition was attenuated by prior incubation with PKG antagonist or expression of IRAGΔE12(GFP) (supplemental Fig. 1, *B* and *C*). Oscillations initiated by activation of the B cell receptor, and thus the endogenous signaling pathway, were similarly inhibited by PKG activation in cells expressing full-length but not truncated IRAG (supplemental Fig. 1, *D* and *E*).

In cells stably expressing InsP$_3$R-3 and transiently expressing M3R, PKG1β, and IRAG(GFP), activation of PKG resulted in an attenuation of CCh-induced Ca^{2+} release (Fig. 5, *A* and pooled data in *C*). In comparison with the effects observed on InsP$_3$R-1- and InsP$_3$R-2-induced release, the degree of inhibition was modest but statistically significant in cells expressing InsP$_3$R-3 (compare Fig. 5*C* with Figs. 2*C*, 3*D*, and 4*D*). Although not investigated further, significant differences in the expression level of IRAG(GFP) and PKG1β were not noted in InsP$_3$R-3-expressing cells, and thus a possibility exists that IRAG may not interact as strongly with InsP$_3$R-3 when compared with other subtypes. Nevertheless, the attenuation of Ca^{2+} release was similarly dependent on IRAG and PKG expression and the formation of a tertiary complex with InsP$_3$R-3 (Fig. 5, *B* and pooled data in *C*). Similar to cells expressing InsP$_3$R-2, no PKG effects were observed that were independent of IRAG, and thus direct PKG phosphorylation is unlikely to occur or, if it does occur, is unlikely to be functionally relevant for modulating Ca^{2+} release through InsP$_3$R-3. In summary, IRAG binding and its subsequent phosphorylation by PKG reduces Ca^{2+} release through all InsP$_3$R subtypes. In addition, direct phosphorylation by PKG does not occur or does not have functional implications for the InsP$_3$R-2 or InsP$_3$R-3. An enhancement of Ca^{2+} release is, however, unmasked in the absence of IRAG in cells expressing the S2+ "neuronal" InsP$_3$R-1.

IRAG Expression Inhibits Direct Modulation of InsP$_3$R-1 by PKA—In many cell types, signaling through the cAMP and cGMP pathways coexists. Given that direct phosphorylation by PKA and PKG on InsP$_3$R-1 and the indirect effects of IRAG modulation by PKG are functionally opposite, we next carried out experiments to determine under what conditions the individual pathways are dominant. Fig. 6*A* shows a typical experimental trace, which illustrates the effects of exposure to cBIMPS, a PKA-specific analog of cAMP. As shown previously, activation of PKA results in an ~2–3-fold increase in the peak CCh- induced Ca^{2+} release in cells stably expressing S2− InsP$_3$R-1 (Fig. 6, *A* and pooled data in *E*). Surprisingly, when identical experiments were performed in S2- InsP$_3$R-1 cells expressing IRAG(GFP) and PKG1β, Ca^{2+} release was unaffected by cBIMPS treatment (Fig. 6, *B* and *E*). The binding of IRAG to S2− InsP$_3$R was necessary for rendering the cells refractory to the effects of PKA activation because the anticipated marked enhancement of CCh-induced Ca^{2+} release was observed in cells expressing IRAGΔE12(GFP) and treated with cBIMPS (Fig. 6*C*). In cells initially incubated with cBIMPS, subsequent activation of PKG with PET-cGMP resulted in the expected inhibition of CCh-stimulated Ca^{2+} release (Fig. 6*D*). Identical results were obtained in cells expressing the neuronal S2+ InsP$_3$R-1 (*i.e.* no effect of PKA activation was observed in cells expressing full-length IRAG-(GFP), but the expected enhancement of Ca^{2+} release was readily observed either in cells not expressing IRAG or transfected with IRAGΔE12(GFP)) (supplemental Fig. 2). The lack of effect of PKA activation on S2− InsP$_3$R-1 in cells expressing IRAG, illustrated in Fig. 6, *B* and *D*, has multiple implications. First, it suggests that InsP$_3$R-1 under these conditions is not functionally altered by PKA activation; second, it indicates that, despite Ser^{696} in IRAG being present in a canonical PKA consensus phosphorylation motif, it is not efficiently phosphorylated by PKA. PKA activation, therefore cannot substitute for the effects of PKG1β anchored to IRAG. These data are entirely consistent with experiments in vascular smooth muscle, which show that although 8-bromo-cyclic GMP reduced Ca^{2+} release, cBIMPS neither enhanced nor inhibited Ca^{2+} release in vascular smooth muscle cells (33).

IRAG Expression Attenuates PKA Phosphorylation of InsP$_3$R-1—The lack of functional effect of PKA phosphorylation on InsP$_3$R-1 in cells expressing IRAG could potentially occur because IRAG binding to InsP$_3$R-1 either physically inhibits the phosphorylation of the receptor or, alternatively, hinders the coupling of the phosphorylation event to the enhanced gating of the channel. The former idea was tested by directly monitoring the phosphorylation status of InsP$_3$R-1 with an antibody that recognizes phosphorylated Ser^{1755} in COS-7 cells expressing IRAG. IRAG(GFP) or IRAGΔE12(GFP) expression appeared to decrease the level of expression of InsP$_3$R-1, and thus the -fold change in phos-

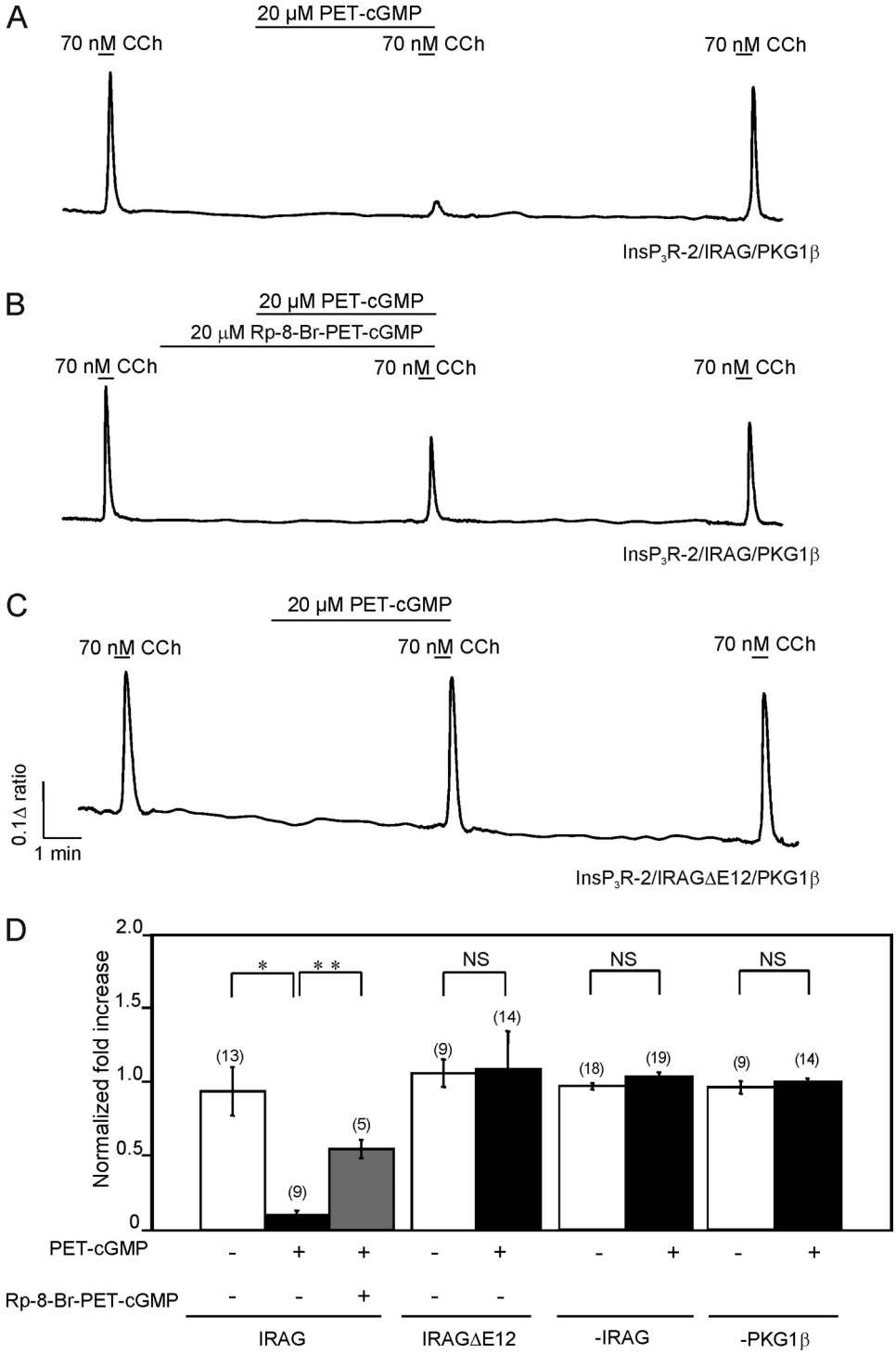

FIGURE 4. **Ca^{2+} release through InsP$_3$R-2 is attenuated by PKG activation in cells expressing IRAG/PKG1β.** DT40-3KO cells stably expressing InsP$_3$R-2 were transfected with cDNA encoding M3R, IRAG(GFP) in *A* and *B* or IRAGΔE12(GFP) in *C*, and PKG1β. In *A*, treatment with 20 μM PET-cGMP resulted in a markedly attenuated CCh-induced Ca^{2+} release in the presence of full-length IRAG. In *B*, this attenuation was significantly reduced by pretreatment with the PKG inhibitor, Rp-8-Br-PET-cGMP. In *C*, no effect of incubation with PET-cGMP was observed in the presence of IRAGΔE12. *D*, pooled data. Data in the *open bars* represent the -fold change of the second response compared with the first response in the absence of treatment. The *filled bars* show the normalized -fold increase of the second peak over the first peak for the indicated experimental condition. *Columns* represent mean ± S.E. (*error bars*). **, $p < 0.0001$; ***, $p < 0.05$; *NS*, not statistically significant. The number of cells in each condition is indicated in *parentheses*.

phorylation in each treatment group was evaluated. Exposure of cells transfected with InsP$_3$R-1 to a PKA-activating mixture of forskolin and isobutylmethylxanthine resulted in robust phosphorylation of S2− InsP$_3$R-1 (Fig. 7*A*, compare *lanes 1* and *2*, and pooled data) and S2+ InsP$_3$R-1 (Fig. 7*B*, *lanes 1* and *2*, and pooled data). The extent of phosphorylation was markedly reduced in cells expressing IRAG (Fig. 7, *A* (*lanes 3* and *4*) and *B* for S2− and S2+ InsP$_3$R-1, respectively, and pooled data). The increase in phosphorylation was at least partially restored in cells expressing IRAGΔE12(GFP) (Fig. 7,

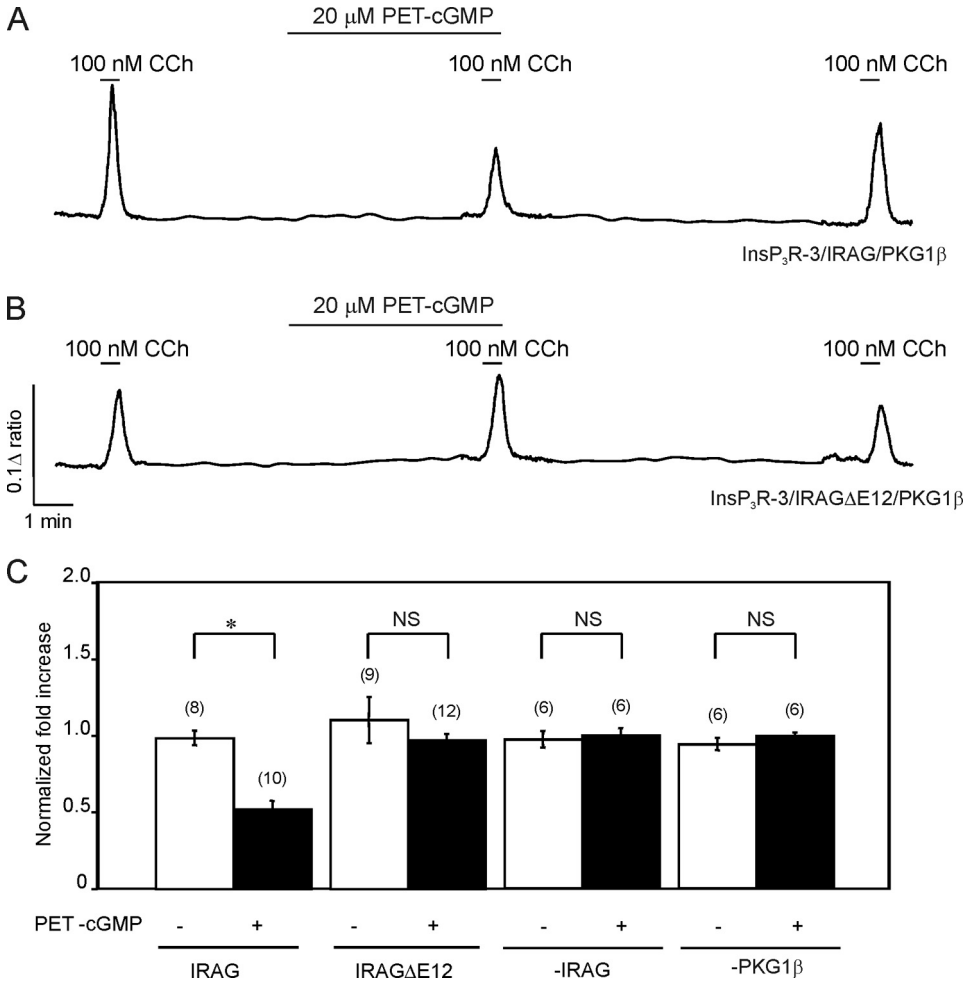

FIGURE 5. **Ca^{2+} release through InsP$_3$R-3 is attenuated by PKG activation in cells expressing IRAG/PKG1β.** DT40-3KO cells stably expressing InsP$_3$R-3 were transfected with cDNA encoding M3R, IRAG(GFP) in *A* or IRAGΔE12(GFP) in *B*, and PKG1β. In *A*, treatment with 20 μM PET-cGMP resulted in a markedly attenuated CCh-induced Ca^{2+} release in the presence of full-length IRAG. In *B*, no effect of incubation with PET-cGMP was observed in the presence of IRAGΔE12. *C*, pooled data. Data in the *open bars* represent the -fold change of the second response compared with the first response in the absence of treatment. The *filled bars* show the normalized -fold increase of the second peak over the first peak for the indicated experimental condition. *Columns* represent mean ± S.E. (*error bars*). *, $p < 0.0001$; *NS*, not statistically significant. The number of cells in each condition is indicated in *parentheses*.

A (*lanes 5* and *6*) and *B* for S2− and S2+ InsP$_3$R-1, respectively, and pooled data). These data are consistent with the idea that IRAG binding to InsP$_3$R-1 reduces the PKA-dependent direct phosphorylation of the receptor and subsequent potentiation of Ca^{2+} release but does not rule out a contribution by other mechanisms.

IRAG Does Not Impact PKA Regulation of InsP$_3$R-2 Unless Phosphorylated by PKG—Next, we addressed whether IRAG expression impacts PKA modulation of InsP$_3$R-2 in a similar fashion to InsP$_3$R-1. A typical example of the effect of PKA activation on InsP$_3$R-2 is shown in Fig. 8*A*, in which a threshold response to M3R stimulation is significantly enhanced following incubation with cBIMPS (12). In contrast to cells expressing InsP$_3$R-1, transfection with IRAG did not alter the effect of PKA activation on Ca^{2+} release via InsP$_3$R-2 (Fig. 8, *B* and pooled data in E). These data indicate that the binding of IRAG to InsP$_3$R-2 does not itself alter receptor phosphorylation and may reflect the fact that the phosphorylation sites in the individual InsP$_3$R subtypes are distinct and physically distant in the receptor's linear sequence (12). This idea was confirmed experimentally by monitoring the phosphorylation of InsP$_3$R-2 in COS-7 cells transiently expressing InsP$_3$R-2 and IRAG constructs. Using an antibody that recognizes phosphorylated Ser^{937} in InsP$_3$R-2, robust receptor phosphorylation following PKA activation was detected in cells expressing IRAG(GFP) and IRAGΔE12(GFP) but not in cells expressing a mutant InsP$_3$R-2 in which the phosphorylation site at serine 937 was mutated to alanine (S937A) (supplemental Fig. 3).

Finally, experiments were performed to determine if the indirect modulation of InsP$_3$R-2 activity following PKG phosphorylation of IRAG could overcome the direct modulation of InsP$_3$R-2 activity following Ser^{937} phosphorylation. The potentiating action of PKA activation could be maintained during repetitive exposure to cBIMPS and subsequent challenge with CCh (Fig. 9*A*). In contrast, when PKA and PKG were activated concurrently, a marked inhibition of the PKA-enhanced Ca^{2+} signal was observed (Fig. 9*B*), indicating that the phosphorylation of IRAG exerts a dominant effect over direct InsP$_3$R-2 phosphorylation.

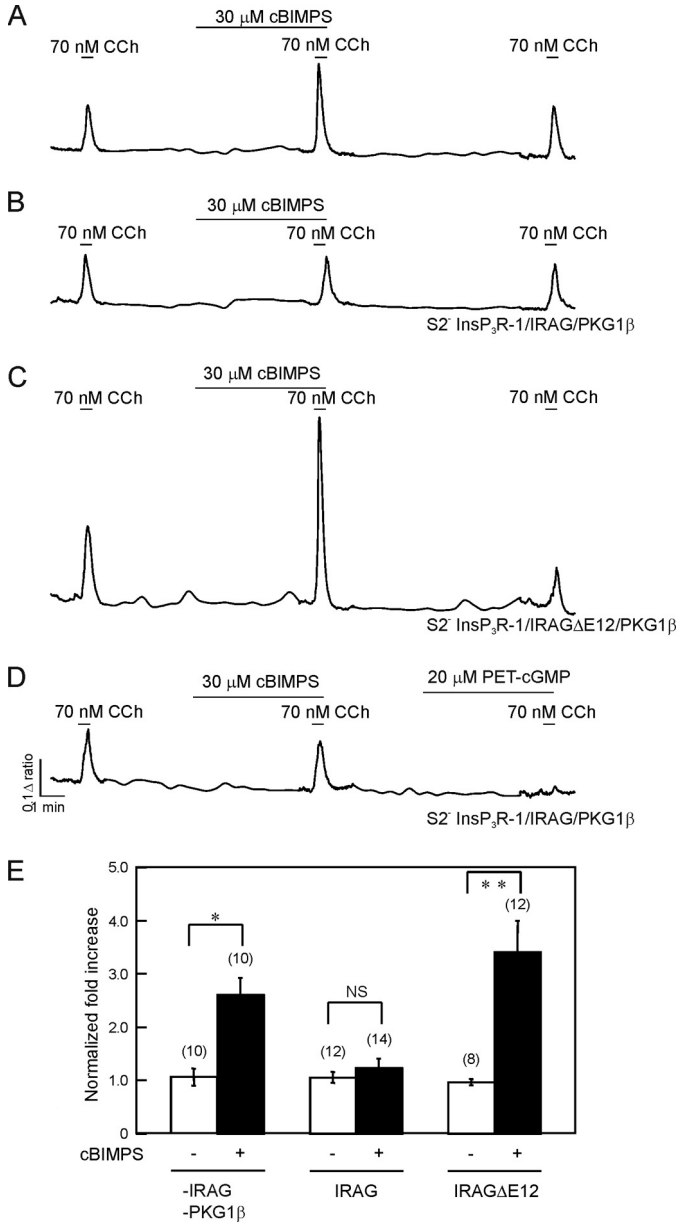

FIGURE 6. **PKA activation fails to enhance Ca^{2+} release through S2-InsP$_3$R-1 in the presence of IRAG/PKG1β.** DT40-3KO cells stably expressing S2− InsP$_3$R-1 were transfected with cDNA encoding M3R and IRAG(GFP) in *B* and *D* or IRAGΔE12(GFP) in *C*, together with PKG1β in *B* and *C*. In *A*, treatment with 30 μM cBIMPS resulted in a significantly enhanced CCh-induced Ca^{2+} release in the absence of IRAG and PKG1β. In *B*, no effect of cBIMPS treatment was observed in cells expressing full-length IRAG. In *C*, cBIMPS incubation resulted in a markedly enhanced CCh-induced Ca^{2+} release in cells expressing IRAGΔE12(GFP). In *D*, cBIMPS treatment did not alter CCh-induced Ca^{2+} release; however, subsequent incubation with the cGMP analog PET-cGMP resulted in significant attenuation of Ca^{2+} release. *E*, pooled data. Data in the *open bars* represent the -fold change of the second response compared with the first response in the absence of treatment. The *filled bars* show the normalized -fold increase of the second peak over the first peak for the indicated experimental condition. *Columns* represent mean ± S.E. (*error bars*). *, $p < 0.001$; ****, $p < 0.01$; *NS*, not statistically significant. The number of cells in each condition is indicated in *parentheses*.

DISCUSSION

Regulation of InsP$_3$R activity following activation of PKG and PKA has been extensively studied (for reviews, see Refs. 11 and 37). It is clear that PKA can directly phosphorylate all InsP$_3$R subtypes, whereas PKG has been shown to phosphorylate the InsP$_3$R-1. PKA activation has generally been reported to increase InsP$_3$R activity(15, 16, 20, 31, 38–40). In contrast, increasing PKG activity has typically been reported to decrease InsP$_3$R-dependent Ca^{2+} release (22, 24, 41), a prominent exception being in hepatocytes, where PKG activation results in phosphorylation of InsP$_3$R-1 at a shared PKA site and raising cGMP enhances agonist-stimulated Ca^{2+} signals (42). In the present study, we have used the DT-40 InsP$_3$R null expression system to define the functional effects of PKG activation, both directly and indirectly through IRAG on each InsP$_3$R subtype in unambiguous isolation. In addition, these studies also provide insight into the interplay between the PKA and PKG signaling modules and the molecular mechanisms that dictate which pathway dominates regulation of InsP$_3$R activity when the pathways are activated together.

In the absence of IRAG expression, raising cGMP levels had no effect on Ca^{2+} release in cells expressing S2− InsP$_3$R-1, InsP$_3$R-2, or InsP$_3$R-3. Because phosphorylation of InsP$_3$R-2 by PKA markedly enhances Ca^{2+} release (12), these data would suggest that serine 937 in InsP$_3$R-2 is not a substrate for PKG. In addition, it is unlikely that any additional, functionally important PKG sites are present in these receptors, leaving the neuronal form of InsP$_3$R-1 as the primary splice variant with potential to be directly regulated by PKG. Of note, a significant proportion of neuronal InsP$_3$R-1 are phosphorylated at Ser^{1755} in an activity-dependent and region-specific manner (30), and it is possible that this results at least partially from PKG activity. Ser^{1755} is the major phosphorylated residue in the brain (43), and analysis of non-phosphorylatable (Ser → Ala) or phosphomimetic (Ser → Glu) mutations at these sites in the context of S2+ InsP$_3$R clearly indicates that only phosphorylation of Ser^{1755} has functional consequences (20, 31). Paradoxically, PKG has, however, been shown to be predominantly, if not exclusively, phosphorylated at Ser^{1589} in S2+ InsP$_3$R-1 (44, 45). Thus, it remains to be established if direct phosphorylation of Ser^{1755} in S2+ InsP$_3$R by PKG occurs and is thus physiologically relevant.

This study demonstrates that IRAG binds to all InsP$_3$R subtypes and can form the basis of a tertiary complex with PKG1β. Phosphorylation of IRAG by PKG1β leads to inhibitory modulation of Ca^{2+} release through each InsP$_3$R subtype and would be predicted to influence Ca^{2+} release in cells where the other components of the complex are expressed. Only a limited amount of information is available regarding the expression of IRAG outside of platelets and tissues/organs with a smooth muscle component (46). In these systems, InsP$_3$R-1 is the predominant subtype expressed, although in platelets, InsP$_3$R-2 is present (47). Smooth muscle of various origins also expresses variable amounts of both InsP$_3$R-2 and InsP$_3$R-3. Notably, the complement and relative amounts of each isoform have been reported to change in proliferative states of smooth muscle (48). IRAG is expressed in various regions of the brain (46) and in osteoclasts (49), and in these cells, if IRAG and PKG1β

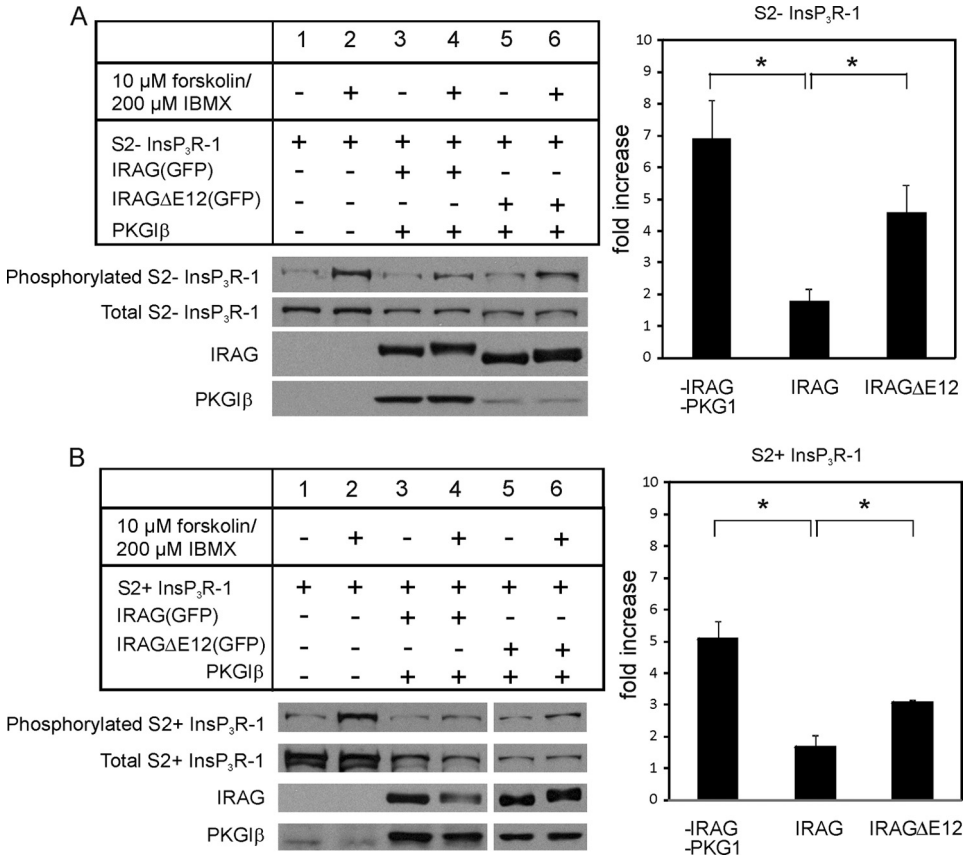

FIGURE 7. **IRAG expression reduces PKA-induced phosphorylation of S2−/S2+ InsP$_3$R-1.** COS-7 cells were transfected with cDNA encoding S2− InsP$_3$R-1 in *A* or S2+ InsP$_3$R-1 in *B*, together with IRAG(GFP) or IRAGΔE12(GFP) and PKG1β. Analysis of phospho-InsP$_3$R band densities for three experiments is shown in the *right-hand panels* for each splice variant; although the expression level of InsP$_3$R was reduced by the transfection of IRAG, the amount of InsP$_3$R when analyzed in each treatment group was not significantly different, and thus the -fold change in each group is shown. Cells were treated with 10 μM forskolin and 200 μM isobutylmethylxanthine for 10 min at room temperature prior to cell lysis. Protein was subjected to SDS-PAGE and then Western blotting for the indicated proteins. Phosphorylation of S2− InsP$_3$R-1 in *A* and S2+ InsP$_3$R-1 in *B* was diminished in the presence of full-length IRAG (compare *lanes 1* and *2* with *lanes 3* and *4*). In contrast, the extent of phosphorylation was largely unaltered by expression of IRAGΔE12(GFP) (*lanes 5* and *6*). *Error bars*, S.E, $p < 0.05$.

are coexpressed, PKG regulation of Ca^{2+} release would be predicted to occur.

In smooth muscle cells, elevating either cAMP or cGMP results in muscle relaxation. The importance of PKG regulation of IRAG and its interaction with InsP$_3$R in this process is clear. For example, deletion of IRAG results in defective regulation by NO of smooth muscle tone (50). In addition, highlighting the importance of "targeting," an identical phenotype was reported when exon 12, encoding the InsP$_3$R interaction domain of IRAG was deleted (25, 33). In contrast, the effects of elevating cAMP in smooth muscle are generally explained either by direct or indirect activation of PKG (51, 52) and phosphorylation of the contractile machinery (53). The effects of cAMP are therefore inconsistent with any role of direct phosphorylation of InsP$_3$R by PKA. Our studies may provide a mechanism to reconcile why IRAG regulation of InsP$_3$R dominates any modulation by direct receptor phosphorylation. These data indicate that the simple expression of IRAG appears to attenuate PKA phosphorylation of InsP$_3$R-1 and negate any functional effects on Ca^{2+} release. Because attenuation of direct PKA regulation requires IRAG binding to InsP$_3$R-1, it is reasonable to suggest that the interaction of the proteins hinders PKA access to the phosphorylation sites at Ser^{1589} and Ser^{1755}. Further studies defining the sites of interaction on each InsP$_3$R for IRAG are necessary to confirm this idea. Our findings also show that signaling via InsP$_3$R-2 is potentially more versatile because, in the presence of IRAG expression, both PKA and PKG modulation can occur and exert opposing effects on Ca^{2+} release. Nevertheless, even in the continued presence of a PKA activator, regulation by cGMP through IRAG predominates and can overcome the enhanced activity initiated by direct receptor phosphorylation.

In summary, the present study adds to our understanding of the cross-talk between signaling pathways that interact at the level of regulation of Ca^{2+} release. Specifically, we have defined the effects on Ca^{2+} release of PKG and PKA activation through each InsP$_3$R subtype in the presence or absence of IRAG expression. This work effectively establishes a set of basic "rules" that can be used to predict the effect of PKA and PKG activation, alone and concurrently, on InsP$_3$-induced Ca^{2+} release, in particular cells expressing various complements of InsP$_3$R subtypes and IRAG/PKG1β. Further testing of these predictions will involve defining in detail the expression profile of IRAG and

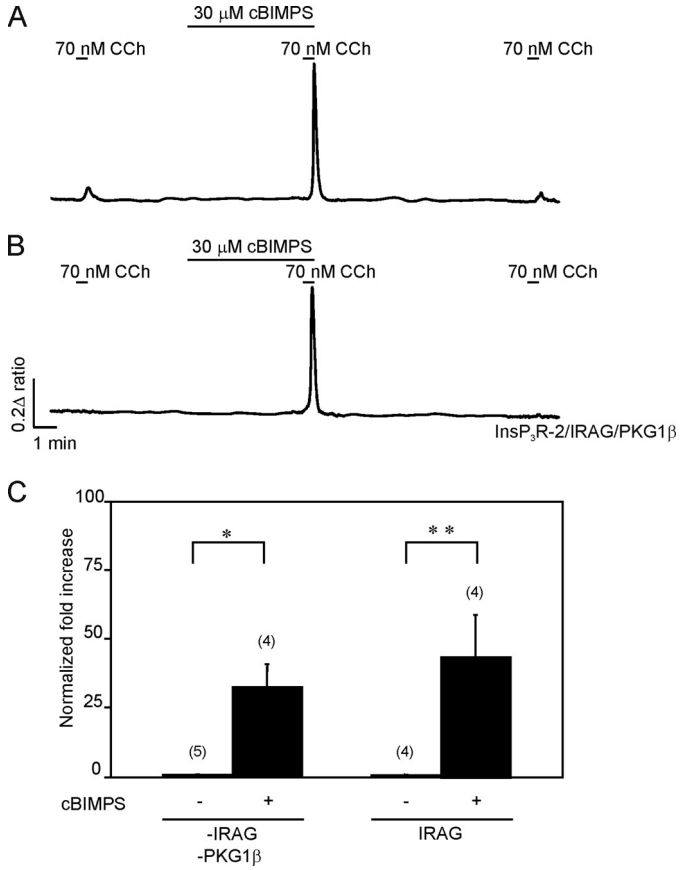

FIGURE 8. **PKA activation enhances Ca^{2+} release through InsP$_3$R-2 in the presence of IRAG/PKG1β.** DT40-3KO cells stably expressing InsP$_3$R-2 were transfected with cDNA encoding M3R in *A* or IRAG(GFP) and PKG1β in *B*. In *A*, treatment with the PKA activator cBIMPS resulted in a marked enhancement of CCh-induced Ca^{2+} release. In *B*, expression of full-length IRAG did not alter the effect of PKA activation. *C*, pooled data. Data are expressed as the normalized -fold increase of the second peak over the first peak. *Columns* represent mean ± S.E. (error bars). **, $p < 0.01$; ****, $p < 0.05$. The number of cells in each condition is indicated in *parentheses*.

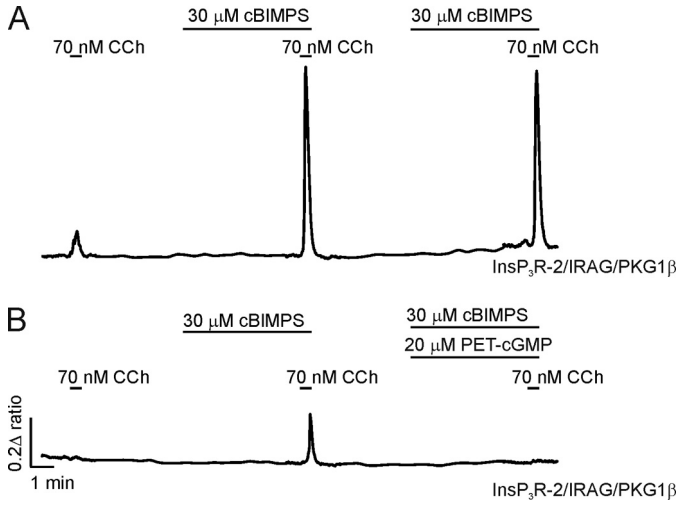

FIGURE 9. **IRAG phosphorylation by PKG exerts a dominant effect over PKA phosphorylation of InsP$_3$R-2.** DT40-3KO cells stably expressing InsP$_3$R-2 were transfected with cDNA encoding M3R, IRAG(GFP), and PKG1β. In *A*, treatment with the PKA activator cBIMPS resulted in a marked enhancement of CCh-induced Ca^{2+} release, which was maintained in the continued presence of the agent. In *B*, subsequent activation of PKG in the continued presence of cBIMPS results in the marked attenuation of the CCh-induced Ca^{2+} release. The experiment shown is typical of three others.

PKG1β, followed by manipulation of the levels of the various components in native cells.

Acknowledgments—We thank Jill Thompson for her usual thorough proofreading of the manuscript and Lyndee Knowlton for excellent technical assistance throughout this study.

REFERENCES

1. Berridge, M. J., Bootman, M. D., and Roderick, H. L. (2003) *Nat. Rev. Mol. Cell Biol.* **4,** 517–529
2. Patterson, R. L., Boehning, D., and Snyder, S. H. (2004) *Annu. Rev. Biochem.* **73,** 437–465
3. Conti, M., and Beavo, J. (2007) *Annu. Rev. Biochem.* **76,** 481–511
4. Willoughby, D., and Cooper, D. M. (2007) *Physiol. Rev.* **87,** 965–1010
5. Berridge, M. J., Lipp, P., and Bootman, M. D. (2000) *Nat. Rev. Mol. Cell Biol.* **1,** 11–21
6. Blondel, O., Takeda, J., Janssen, H., Seino, S., and Bell, G. I. (1993) *J. Biol. Chem.* **268,** 11356–11363
7. Furuichi, T., Yoshikawa, S., Miyawaki, A., Wada, K., Maeda, N., and Mikoshiba, K. (1989) *Nature* **342,** 32–38
8. Südhof, T. C., Newton, C. L., Archer, B. T., 3rd, Ushkaryov, Y. A., and Mignery, G. A. (1991) *EMBO J.* **10,** 3199–3206
9. Foskett, J. K., White, C., Cheung, K. H., and Mak, D. O. (2007) *Physiol. Rev.* **87,** 593–658
10. Patel, S., Joseph, S. K., and Thomas, A. P. (1999) *Cell Calcium* **25,** 247–264
11. Yule, D. I., Betzenhauser, M. J., and Joseph, S. K. (2010) *Cell Calcium* **47,** 469–479
12. Betzenhauser, M. J., Fike, J. L., Wagner, L. E., 2nd, and Yule, D. I. (2009) *J. Biol. Chem.* **284,** 25116–25125
13. Ferris, C. D., Cameron, A. M., Bredt, D. S., Huganir, R. L., and Snyder, S. H. (1991) *Biochem. Biophys. Res. Commun.* **175,** 192–198
14. Soulsby, M. D., and Wojcikiewicz, R. J. (2005) *Biochem. J.* **392,** 493–497
15. Tang, T. S., Tu, H., Wang, Z., and Bezprozvanny, I. (2003) *J. Neurosci.* **23,** 403–415
16. Wagner, L. E., 2nd, Joseph, S. K., and Yule, D. I. (2008) *J Physiol* **586,** 3577–3596
17. Soulsby, M. D., and Wojcikiewicz, R. J. (2007) *Cell Calcium* **42,** 261–270
18. Bruce, J. I., Shuttleworth, T. J., Giovannucci, D. R., and Yule, D. I. (2002) *J. Biol. Chem.* **277,** 1340–1348
19. Hofmann, F., Bernhard, D., Lukowski, R., and Weinmeister, P. (2009) *Handb. Exp. Pharmacol.* **191,** 137–162
20. Wagner, L. E., 2nd, Li, W. H., and Yule, D. I. (2003) *J. Biol. Chem.* **278,** 45811–45817
21. Cavallini, L., Coassin, M., Borean, A., and Alexandre, A. (1996) *J. Biol. Chem.* **271,** 5545–5551
22. Komalavilas, P., and Lincoln, T. M. (1994) *J. Biol. Chem.* **269,** 8701–8707
23. Quinton, T. M., Brown, K. D., and Dean, W. L. (1996) *Biochemistry* **35,** 6865–6871
24. Tertyshnikova, S., Yan, X., and Fein, A. (1998) *J. Physiol.* **512,** 89–96
25. Antl, M., von Brühl, M. L., Eiglsperger, C., Werner, M., Konrad, I., Kocher, T., Wilm, M., Hofmann, F., Massberg, S., and Schlossmann, J. (2007) *Blood* **109,** 552–559
26. Schlossmann, J., Ammendola, A., Ashman, K., Zong, X., Huber, A., Neubauer, G., Wang, G. X., Allescher, H. D., Korth, M., Wilm, M., Hofmann, F., and Ruth, P. (2000) *Nature* **404,** 197–201
27. Ammendola, A., Geiselhöringer, A., Hofmann, F., and Schlossmann, J. (2001) *J. Biol. Chem.* **276,** 24153–24159
28. Giovannucci, D. R., Groblewski, G. E., Sneyd, J., and Yule, D. I. (2000) *J. Biol. Chem.* **275,** 33704–33711
29. Betzenhauser, M. J., Wagner, L. E., 2nd, Iwai, M., Michikawa, T., Mikoshiba, K., and Yule, D. I. (2008) *J. Biol. Chem.* **283,** 21579–21587
30. Pieper, A. A., Brat, D. J., O'Hearn, E., Krug, D. K., Kaplin, A. I., Takahashi, K., Greenberg, J. H., Ginty, D., Molliver, M. E., and Snyder, S. H. (2001) *Neuroscience* **102,** 433–444

31. Wagner, L. E., 2nd, Li, W. H., Joseph, S. K., and Yule, D. I. (2004) *J. Biol. Chem.* **279,** 46242–46252
32. Betzenhauser, M. J., Wagner, L. E., 2nd, Won, J. H., and Yule, D. I. (2008) *Methods* **46,** 177–182
33. Geiselhöringer, A., Werner, M., Sigl, K., Smital, P., Wörner, R., Acheo, L., Stieber, J., Weinmeister, P., Feil, R., Feil, S., Wegener, J., Hofmann, F., and Schlossmann, J. (2004) *EMBO J.* **23,** 4222–4231
34. Boehning, D., and Joseph, S. K. (2000) *J. Biol. Chem.* **275,** 21492–21499
35. Sugawara, H., Kurosaki, M., Takata, M., and Kurosaki, T. (1997) *EMBO J.* **16,** 3078–3088
36. Betzenhauser, M. J., Wagner, L. E., 2nd, Park, H. S., and Yule, D. I. (2009) *J. Biol. Chem.* **284,** 16156–16163
37. Vanderheyden, V., Devogelaere, B., Missiaen, L., De Smedt, H., Bultynck, G., and Parys, J. B. (2009) *Biochim. Biophys. Acta* **1793,** 959–970
38. Nakade, S., Rhee, S. K., Hamanaka, H., and Mikoshiba, K. (1994) *J. Biol. Chem.* **269,** 6735–6742
39. Joseph, S. K., and Ryan, S. V. (1993) *J. Biol. Chem.* **268,** 23059–23065
40. Wojcikiewicz, R. J., and Luo, S. G. (1998) *J. Biol. Chem.* **273,** 5670–5677
41. Murthy, K. S., and Zhou, H. (2003) *Am. J. Physiol. Gastrointest. Liver Physiol.* **284,** G221–G230
42. Rooney, T. A., Joseph, S. K., Queen, C., and Thomas, A. P. (1996) *J. Biol. Chem.* **271,** 19817–19825
43. Danoff, S. K., Ferris, C. D., Donath, C., Fischer, G. A., Munemitsu, S., Ullrich, A., Snyder, S. H., and Ross, C. A. (1991) *Proc. Natl. Acad. Sci. U.S.A.* **88,** 2951–2955
44. Haug, L. S., Jensen, V., Hvalby, O., Walaas, S. I., and Ostvold, A. C. (1999) *J. Biol. Chem.* **274,** 7467–7473
45. Soulsby, M. D., Alzayady, K., Xu, Q., and Wojcikiewicz, R. J. (2004) *FEBS Lett.* **557,** 181–184
46. Geiselhöringer, A., Gaisa, M., Hofmann, F., and Schlossmann, J. (2004) *FEBS Lett.* **575,** 19–22
47. Quinton, T. M., and Dean, W. L. (1996) *Biochem. Biophys. Res. Commun.* **224,** 740–746
48. Tasker, P. N., Taylor, C. W., and Nixon, G. F. (2000) *Biochem. Biophys. Res. Commun.* **273,** 907–912
49. Yaroslavskiy, B. B., Turkova, I., Wang, Y., Robinson, L. J., and Blair, H. C. (2010) *Lab. Invest.* **90**(10), 1533–1542
50. Desch, M., Sigl, K., Hieke, B., Salb, K., Kees, F., Bernhard, D., Jochim, A., Spiessberger, B., Höcherl, K., Feil, R., Feil, S., Lukowski, R., Wegener, J. W., Hofmann, F., and Schlossmann, J. (2010) *Cardiovasc. Res.* **86,** 496–505
51. Lincoln, T. M., Cornwell, T. L., and Taylor, A. E. (1990) *Am. J. Physiol.* **258,** C399–C407
52. Murthy, K. S. (2001) *Am. J. Physiol. Gastrointest Liver Physiol.* **281,** G1238–G1245
53. Silver, P. J., and DiSalvo, J. (1979) *J. Biol. Chem.* **254,** 9951–9954